"*Candidatus* Desulfobulbus rimicarensis," an Uncultivated Deltaproteobacterial Epibiont from the Deep-Sea Hydrothermal Vent Shrimp *Rimicaris exoculata*

Jiang Lijing [1, 2, 3, 4], Liu Xuewen [1, 2, 3, 4], Dong Chunming [1, 2, 3, 4], Huang Zhaobin [1, 2, 3, 4], Cambon-Bonavita Marie-Anne [4, 5], Alain Karine [4, 6], Gu Li [1, 2, 3, 4], Wang Shasha [1, 2, 3, 4], Shao Zongze [1, 2, 3, 4, *]

[1] Minist Nat Resources, Key Lab Marine Genet Resources, Inst Oceanog 3, Xiamen, Peoples R China.
[2] State Key Lab Breeding Base Marine Genet Resource, Xiamen, Peoples R China.
[3] Fujian Key Lab Marine Genet Resources, Xiamen, Peoples R China.
[4] Sino French Lab Deep Sea Microbiol MICROBSEA, LIA1211, Xiamen, Peoples R China.
[5] Univ Brest, LM2E, CNRS, IFREMER, Plouzane, France.
[6] Univ Brest, LM2E, CNRS, IFREMER, Plouzane, France.

* Corresponding author : Zongze Shao , email address : shaozz@163.com

Abstract :

The deep-sea hydrothermal vent shrimp Rimicaris exoculata largely depends on a dense epibiotic chemoautotrophic bacterial community within its enlarged cephalothoracic chamber. However, our understanding of shrimp-bacterium interactions is limited. In this report, we focused on the deltaproteobacterial epibiont of R. exoculata from the relatively unexplored South Mid-Atlantic Ridge. A nearly complete genome of a Deltaproteobacteria epibiont was binned from the assembled metagenome. Whole-genome phylogenetic analysis reveals that it is affiliated with the genus Desulfobulbus, representing a potential novel species for which the name "Candidatus Desulfobulbus rimicarensis" is proposed. Genomic and transcriptomic analyses reveal that this bacterium utilizes the Wood-Ljungdahl pathway for carbon assimilation and harvests energy via sulfur disproportionation, which is significantly different from other shrimp epibionts. Additionally, this epibiont has putative nitrogen fixation activity, but it is extremely active in directly taking up ammonia and urea from the host or vent environments. Moreover, the epibiont could be distinguished from its free-living relatives by various features, such as the lack of chemotaxis and motility traits, a dramatic reduction in biosynthesis genes for capsular and extracellular polysaccharides, enrichment of genes required for carbon fixation and sulfur metabolism, and resistance to environmental toxins. Our study highlights the unique role and symbiotic adaptation of Deltaproteobacteria in deep-sea hydrothermal vent shrimps.

IMPORTANCE

The shrimp Rimicaris exoculata represents the dominant faunal biomass at many deep-sea hydrothermal vent ecosystems along the Mid-Atlantic Ridge. This organism harbors dense bacterial epibiont communities in its enlarged cephalothoracic chamber that play an important nutritional role. Deltaproteobacteria are ubiquitous in epibiotic communities of R. exoculata, and their functional roles as

epibionts are based solely on the presence of functional genes. Here, we describe "Candidatus Desulfobulbus rimicarensis," an uncultivated deltaproteobacterial epibiont. Compared to campylobacterial and gammaproteobacterial epibionts of R. exoculata, this bacterium possessed unique metabolic pathways, such as the Wood-Ljungdahl pathway, as well as sulfur disproportionation and nitrogen fixation pathways. Furthermore, this epibiont can be distinguished from closely related free-living Desulfobulbus strains by its reduced genetic content and potential loss of functions, suggesting unique adaptations to the shrimp host. This study is a genomic and transcriptomic analysis of a deltaproteobacterial epibiont and largely expands the understanding of its metabolism and adaptation to the R. exoculata host.

INTRODUCTION

The shrimp *Rimicaris exoculata* (Williams and Rona, 1986) dominates the macrofauna at many hydrothermal vent sites along the Mid-Atlantic Ridge (MAR), aggregating around active hydrothermal vent chimneys in the mixing zone between electron donor-rich hydrothermal fluids and the surrounding cold oxygenated seawater. Densities of up to 3,000 individuals per m^2 were observed (Schmidt, 2008). *R. exoculata* harbors high concentrations of epibiotic bacteria on the inner side of the enlarged cephalothoracic chamber and modified mouthparts, highlighting a symbiosis between the shrimp and its epibionts (Polz and Cavanaugh, 1995; Zbinden et al., 2004; Zbinden et al., 2008; Petersen et al., 2010). A number of studies have focused on the nature of this association and its benefits for the shrimp, which have suggested that the shrimp mainly obtains organic matter from epibiotic bacteria that inhabit the cephalothoracic chamber rather than by grazing on free-living bacteria that are associated with chimney walls (Van Dover, 1988; Rieley et al., 1999; Gebruk et al., 2000; Zbinden et al., 2008). Furthermore, both inorganic carbon fixation by these chemosynthetic epibionts and transtegumental absorption of dissolved organic matter from epibionts to the shrimp have been demonstrated using isotope-labeling experiments (Ponsard et al., 2013).

Recent studies have demonstrated that *R. exoculata* epibiotic communities consist of a high diversity of *Campylobacteria* (previously *Epsilonproteobacteria)*, *Gammaproteobacteria*, *Deltaproteobacteria*, *Alphaproteobacteria*, *Zetaproteobacteria*, *Betaproteobacteria* and *Bacteroidetes* (Petersen et al., 2010; Hugler et al., 2011; Guri et al., 2012; Jan et al., 2014). Growth of the epibiotic chemolithoautotrophs can be driven by a variety of electron sources, such as reduced sulfur compounds, molecular hydrogen, methane and iron (Zbinden et al., 2008; Petersen et al., 2010; Hugler et al., 2011; Guri et al., 2012; Jan et al., 2014). Based on a functional gene survey, two carbon fixation pathways have been highlighted in the epibiotic communities in *R. exoculata* cephalothoracic chambers, namely, the reductive tricarboxylic acid (rTCA) cycle and the Calvin–Benson–Bassham (CBB) cycle (Hugler et al., 2011). A recent metagenomic study performed on a shrimp from the Rainbow hydrothermal vent field revealed that the rTCA and CBB cycles were used for carbon fixation by two filamentous epibionts belonging to the *Campylobacteria* and the *Gammaproteobacteria*, respectively. These epibionts could couple the

85   oxidation of reduced sulfur compounds or molecular hydrogen to oxygen or nitrate reduction (Jan

86   et al., 2014). In addition, synthetic products from epibiotic chemoautotrophy, such as amino acids,

87   sugars, and vitamins, could be transferred to the shrimp (Jan et al., 2014).

88   Meta-omics methods are very useful in adequately identifying and investigating epibiont

89   genetic potential, as most symbiotic bacteria are resistant to *in vitro* cultivation. An early report on

90   *R. exoculata* epibionts provided the first insights into potential metabolisms of the epibionts, based

91   on three genomic bins belonging to *Gammaproteobacteria*, *Campylobacteria* and

92   *Zetaproteobacteria* (Jan et al., 2014). However, these three genome sequences were incomplete

93   and their complete metabolic relationships could not be reconstructed, thereby preventing the

94   interactions with the shrimp host to be predicted. In addition to *Campylobacteria* and

95   *Gammaproteobacteria*, *Deltaproteobacteria* are also frequently detected in epibiotic communities

96   of *R. exoculata* from different deep-sea hydrothermal sites, as revealed by 16S rRNA gene

97   sequencing, fluorescence *in situ* hybridization (FISH), and metagenomic analysis (Hugler et al.,

98   2011; Guri et al., 2012; Jan et al., 2014). For example, *Deltaproteobacteria* were highly

99   represented in clone libraries of shrimp epibionts from the Snake Pit hydrothermal vent field

100   (Hugler et al., 2011), and were present in nearly all the life stages of the shrimp at the Logachev

101   vent site (Guri et al., 2012). These studies tend to indicate that *Deltaproteobacteria* might play a

102   role in shrimp-epibiont interactions. Moreover, Hugler *et al.* proposed that these epibionts could

103   perform sulfate reduction or sulfur disproportionation only based on the presence of functional

104   genes—the *aprA* gene coding for 5'-adenylylsulfate reductase and the *hynL* gene encoding the

105   large subunit of a [NiFe] hydrogenase (Hugler et al., 2011). Therefore, the ecological functions

106   and potential benefits to the shrimp host remain poorly understood so far, largely due to a lack of

107   genome-level investigations.

108   In this study, we investigated the *Deltaproteobacteria* associated with cephalothoracic

109   chamber of shrimps sampled from a new hydrothermal vent field named "Deyin," in the South

110   Mid-Atlantic Ridge (SMAR). Using integrated metagenomics and metatranscriptomics, we

111   assembled and binned the genome of a novel species called *Candidatus* Desulfobulbus

112   rimicarensis, which represents a draft genome of uncultivated deltaproteobacterial epibiont of a

113   deep-sea hydrothermal vent shrimp. Then, we investigated the evolutionary relationships,

114   metabolic activity, and functional dissimilarity of *Candidatus* Desulfobulbus rimicarensis in

115   relation to closely related free-living *Desulfobulbus* strains in order to decipher its adaptation to

116   the shrimp host and to understand the shrimp-epibiont partnership.

117

RESULTS AND DISCUSSION

Abundance and Localization of the family *Desulfobulbaceae*. In order to assess the microbial diversity of *R. exoculata* epibionts, nine adult shrimp individuals sampled from the SMAR (Fig. S1) were analyzed by 454 high-throughput pyrosequencing. No obvious differences in microbial community structures were observed among individuals. The epibiotic bacteria mainly consist of *Campylobacteria*, *Gammaproteobacteria*, *Deltaproteobacteria* and *Bacteroidetes* (Fig. S2) (Dong et al., 2019). *Deltaproteobacteria* accounted for 0.9 to 4.5% of the epibiotic community of the *R. exoculata* individuals, and *Desulfobulbaceae* accounted for 81.5%-97.9% of the *Deltaproteobacteria* taxa. FISH was also performed to explore the presence of *Desulfobulbaceae* on the cephalothorax sections of the shrimp (Fig. S3). The general probe DSB706 (Manz, 1992), which targets most *Desulfobulbaceae* species, was used, revealing *Desulfobulbaceae* cells at the base of the setae, as previously observed in *R. exoculata* from deep-sea hydrothermal vent sites at the Mid-Atlantic Ridge (Hugler et al., 2011). These *Deltaproteobacteria* were directly attached to the scaphognathite seta, as well as nearby the long filamentous bacteria affiliated to *Campylobacteria* or *Gammaproteobacteria*. This specific localization indicates that *Desulfobulbaceae* are not opportunistic. In addition, *Desulfobulbaceae* species were positively identified by FISH in all tested individuals (*n*= 3). In this study, a total of 16 shrimps were utilized for the various analyses that were performed using 16S rRNA gene amplicon sequencing, FISH, metagenomics, and metatranscriptomics. In all 16 shrimp individuals, *Desulfobulbaceae* bacteria were found as residents of the epibiotic community of the cephalothoracic chamber, indicating that, at the SMAR hydrothermal field, these bacteria were regular epibionts in the *R. exoculata* cephalothoracic chamber.

Genome assembly, characteristics and phylogeny of *Desulfobulbaceae*. *De novo* metagenomic assembly and then binning based on compositional features (tetranucleotide signatures (Fig. S4) and G+C content), followed by alignment, which resulted in several genomic bins. The genomic bin affiliated to *Desulfobulbaceae*, named DR15, was chosen for further analysis. Genome completeness was estimated to be 95.65% and to have only 0.2% contamination based on the checkM method, indicating that the draft genome had a high level of completeness.

147   In order to determine the taxonomic position of DR15, a maximum-likelihood phylogenetic tree

148   was constructed based on 92 concatenated core genes. The result revealed that strain DR15 was

149   affiliated to the genus *Desulfobulbus*, forming a separate branch with three

150   metagenome-assembled genomes (MAGs) from hydrothermal venting fluids, in the phylogenetic

151   tree (Fig. S5).

152   The draft genome consisted of 295 contigs (2,921,535 base pairs in length), with an average

153   G+C content of 47.3 mol% (Fig. 1 and Table 1). The genome contained a total of 2,882

154   protein-coding DNA sequences, resulting in an 83.7% coding density. Approximately two-thirds

155   (1,808) of the protein-coding genes in the genome had the highest BLAST scores against

156   *Deltaproteobacteria* genomes. Of these genes, the majority (81.5%) matched against the family

157   *Desulfobulbaceae,* and 886 coding DNA sequences had top hits with genes of *Desulfobulbus*

158   species. Compared to the genomes of its closest free-living relatives, including *Desulfobulbus*

159   *mediterraneus* DSM 13871, *Desulfobulbus japonicus* DSM 18378 and *Desulfobulbus propionicus*

160   DSM 2032 (feature summary for these 3 genomes: size, 3.9–5.8 Mb; G+C content, 45.8–58.9

161   mol%; coding density, 83.4–88.3%), DR15 had the smallest genome size and possessed lower

162   coding density than *D. mediterraneus* DSM 13871 and *D. propionicus* DSM 2032 (Table 1). The

163   genomic size of DR15 was reduced 24–50% compared to the closest related strains. The genome

164   of DR15 had low values of average nucleotide identity (ANI) when compared with genomes of its

165   closest relatives; the highest match was with *D. mediterraneus* DSM 13871 with 66.77% ANI,

166   followed by *D. japonicus* DSM 18378 (66.62%) and *D. propionicus* DSM 2032 (66.53%) (Table

167   1). These associations are all far below the threshold ANI value of 94–96% for species delineation

168   (Richter and Rosselló-Mora, 2009), suggesting that strain DR15 represents a novel species.

169   Combining the above data, we propose that DR15 should be assigned as a novel species of

170   the genus *Desulfobulbus*, named *Candidatus* Desulfobulbus rimicarensis. Strain DR15 is a

171   deltaproteobacterial representative of the epibionts of this deep-sea hydrothermal vent shrimp.

172

173   **Metabolism.** Integrated metagenomic and metatranscriptomic analyses were used to decipher

174   the metabolic potential and transcriptional activity (RNA expression) of *Candidatus*

175   Desulfobulbus rimicarensis. Once onboard, live shrimps were immediately frozen in liquid

176   nitrogen. Although we cannot exclude that the expression of the messenger RNAs may have been

177 partially modified during the sample ascent, we have nevertheless an approximation of the

178 expression *in situ*.

Carbon fixation and central carbon metabolism

180 In contrast to the epibiotic chemolithoautotrophs previously described in *R. exoculata*, strain

181 DR15 probably uses the Wood-Ljungdahl (WL) pathway for carbon fixation. The epibiont genome

182 contains nearly the complete set of genes required for WL pathway, including homologs of

183 formate dehydrogenase (*fdhA, fdhD, fdhF*), formyl-tetrahydrofolate (THF) synthetase (*fhs*),

184 methylene-THF dehydrogenase (*folD*), methylene-THF reductase (*metF*), methyltransferase

185 (*acsE*), bifunctional carbon monoxide dehydrogenase/acetyl-CoA synthase (*acsABC*),

186 phosphotransacetylase (*pta*), and acetate kinase (Fig. S6 and Table S1). The *fchA* gene encoding

187 the formyl-THF cyclohydrolase, which is responsible for converting formyl-THF into methyl-THF,

188 was absent in the draft genome. Previous studies suggest that this gene is not essential for the WL

189 pathway (Pierce et al., 2008; Shin et al., 2016). The *metV* gene was also absent; instead, two

190 copies of *metF* gene were found in strain DR15, which could possibly replace the role of MetV in

191 catalyzing the methylenetetrahydrofolate reductase reaction. This agrees with previous studies in

192 *Acetohalobium arabaticum* (Shin et al., 2016), *Thermus thermophilus* (Igari et al., 2011), and

193 *Escherichia coli* (Guenther et al., 1999). In addition, the epibiont genome contained genes

194 encoding for THF biosynthesis, corrinoid iron-sulfur protein, and molybdopterin cofactor, which

195 play key roles in single-carbon transfer for synthesizing acetyl-CoA from carbon dioxide and

196 molecular hydrogen (Schuchmann and Muller, 2014). This suggests that strain DR15 could

197 synthesize these cofactors to meet the requirements of the WL pathway. In addition, the strain

198 DR15 genome possessed nearly all of the genes needed to reconstruct the complete central

199 pathways, such as the TCA cycle, as well as the Embden–Meyerhof–Parnas, pentose phosphate,

200 gluconeogenesis, and methylmalonyl-CoA pathways (Fig. 3 and Table S1).

201 All genes required for carbon fixation and central carbon metabolisms described above were

202 found to be actively transcribed in strain DR15 among the studied samples (Table S1). The genes

203 *acsE*, *fhs*, and *fdhF* for the WL pathway, *gltA* for citrate synthase in TCA cycle, *talA* encoding

204 transaldolase-associated with the pentose phosphate pathway, *actP* for acetate transport, and *porA*

205 for conversion of acetyl-CoA to pyruvate had the highest transcript abundances (Fig. 3 and Table

206 S1). These data indicated that carbon fixation, acetate uptake, the TCA cycle, and pentose

207 phosphate pathway were active in strain DR15, and around 98-99% of the acetyl-CoA synthesized

208 *via* WL pathway could be converted into pyruvate, which links the autotrophic WL pathway to

209 heterotrophic metabolism. In addition, a carbonic anhydrase-encoding gene, functioning as a

210 carbon dioxide-concentrator that elevates inorganic carbon levels for fixation, was highly

211 expressed. These results suggest that this epibiont could be an active chemoautotroph growing by

212 using the WL pathway for carbon fixation.

213   The WL pathway was the only carbon fixation pathway discovered in this bacterium.

214 Previous studies have revealed two other carbon fixation pathways, rTCA cycle and CBB cycle,

215 from the epibiotic chemolithoautotrophs of the same vent shrimp species, collected further north

216 of the Mid-Atlantic ridge (Jan et al., 2014) in epibionts belonging to *Campylobacteria* and

217 *Gammaproteobacteria*. We identified a bacterial symbiont from a vent animal host that is likely to

218 use the WL pathway for carbon fixation. We also report a carbon fixation pathway in a member of

219 the genus *Desulfobulbus.* The pathway has been highlighted in the sulfur-disproportionating

220 bacterium *Desulfocapsa sulfoexigens* (Finster et al. 2013), which is closely related to strain DR15.

221 In addition, most of the enzymes in the WL pathway encoded in the genome of strain DR15 were

222 most closely related to members of *Deltaproteobacteria* (Fig. S7 and S8).We propose that, as a

223 primary producer in the epibiotic community, the WL pathway could compensate for the rTCA

224 and CBB pathways and could support the growth of the dominant vent fauna.

225

226 **Disproportionation of inorganic sulfur compounds**

227 The biological disproportionation of inorganic sulfur compounds is a microbiologically catalyzed

228 chemolithotrophic process, in which sulfur compounds—such as elemental sulfur, thiosulfate and

229 sulfite—serve as both electron donors and acceptors in order to generate hydrogen sulfide and

230 sulfate. The microbes involved in this type of "inorganic fermentation" or "mineral fermentation"

231 are phylogenetically related to several phyla: *Thermodesulfobacteria* (Slobodkin et al., 2012;

232 Kojima et al., 2016), *Firmicutes* (Jackson et al., 2000), *Gammaproteobacteria* (Obraztsova et al.,

233 2002), and *Deltaproteobacteria* (Bak et al., 1987; Finster et al.,1998; Finster, 2008; Slobodkin et

234 al., 2013, 2016; Slobodkina et al., 2016). The latter is generally regarded as a lineage of

235 sulfate-reducers (Finster, 2008). Moreover, the capacity to disproportionate inorganic sulfur

236 compounds is relatively common among sulfate-reducers (Finster, 2008). In this study, we have a

237   hypothesis that *Candidatus* Desulfobulbus rimicarensis grew *via* disproportionation of reduced

238   sulfur compounds, such as thiosulfate, sulfite and elemental sulfur (Fig. 3 and Table S1).

239   Two thiosulfate reductases (encoding by *phsAB*) were found in the strain DR15 genome and

240   could catalyze the initial step of thiosulfate disproportionation, probably by converting thiosulfate

241   into sulfite and hydrogen sulfide (or less likely to sulfite and element sulfur) (Cypionka, 1989;

242   Frederiksen and Finster, 2004). Thereafter, there are two parallel ways for the oxidation of sulfite

243   to sulfate reported in the literature: 1) the sulfate reduction pathway in the reverse direction and 2)

244   the activity of sulfite oxidoreductase (Cypionka, 1989; Finster, 2008). The strain DR15 genome

245   contains the complete pathway for dissimilatory sulfate reduction, including ATP sulfurylase

246   (encoded by the gene *sat*), APS reductase (gene *aprAB*), and dissimilatory sulfite reductase (gene

247   *dsrABCD*). Also, genes encoding the APS reductase-associated electron transfer complex

248   (QmoABC) and dissimilatory sulfite reductase-associated electron transport proteins (DsrMKJOP)

249   are present in this genome (Fig. 2B). However, there are no genes that code for sulfite

250   oxidoreductase (Table S1), indicating that strain DR15 likely uses the reverse sulfate reduction

251   pathway to oxidize sulfite to sulfate during thiosulfate disproportionation. The disproportionation

252   of elemental sulfur can also occur *via* this route, although the first step differs from thiosulfate and

253   is not well described. The capacity to couple growth to the disproportionation of thiosulfate or

254   elemental sulfur has been observed in *Desulfobulbus propionicus* (Lovley and Phillips, 1994;

255   Finster, 2008), a close relative to the epibiont within the *Desulfobulbaceae* family (Fig. S5). In

256   addition, the predominance of *Desulfobulbaceae* members has also been demonstrated in

257   elemental sulfur-disproportionating enrichment cultures (Finster, 2008). Thus, we propose that

258   strain DR15 may be capable of inorganic sulfur compound disproportionation. Furthermore,

259   transcriptomic analysis revealed that all of the genes involved in the disproportionation of reduced

260   sulfur compounds were expressed (Fig. 2A and Table S1). The genes *aprAB* for APS reductase and

261   *sat* encoding ATP sulfurylase had the highest abundances among all transcripts, followed by

262   *phsAB* for thiosulfate reductase and *dsrABCD* for dissimilatory sulfite reductase. These data,

263   including the expression of *phsAB* genes that are not expressed during sulfate-reduction,

264   confirmed that the disproportionation of inorganic sulfur compounds was active. Therefore, it is

265   likely that thiosulfate disproportionation provides energy for the growth of strain DR15. However,

266   it is also possible that the epibiont might grow *via* sulfate-reduction under certain conditions.

267   Previously, the growth of the epibiotic chemolithoautotrophs associated with *R. exoculata*

268   and affiliated to *Gammaproteobacteria*, *Campylobacteria*, *Alphaproteobacteria*, and

269   *Zetaproteobacteria*, was found to be fueled by the oxidation of reduced sulfur compounds,

270   molecular hydrogen, methane, and iron (Zbinden et al., 2008; Petersen et al., 2010; Hugler et al.,

271   2011; Guri et al., 2012; Jan et al., 2014). This study demonstrated that chemoautotrophic epibionts

272   of *R. exoculata* are likely to be powered by the disproportionation of inorganic sulfur compounds.

273   Hugler *et al.* had previously made this assumption based on the detection of *aprA* sequences from

274   *Deltaproteobacteria* during a molecular screening of functional genes (Hugler et al., 2011). In the

275   cephalothoracic chamber, energy production through sulfur compounds disproportionation would

276   prevent competition with co-occurring epibionts for energy sources.

277

Hydrogen oxidation

279   Genomic analysis revealed that the DR15 genome encoded for four [NiFe]-hydrogenases: two

280   periplasmic hydrogenases group 1 (Hya and Hyb), one cytoplasmic, methyl-viologen-reducing

281   hydrogenase (Mvh), and one membrane-associated energy-converting [NiFe] hydrogenase (Ech)

282   (Fig. S9 and Table S1), while no [FeFe]-hydrogenase genes were detected in the draft genome.

283   [NiFe]-hydrogenases Group 1 is a membrane-bound respiratory hydrogenase, performing

284   hydrogen oxidation linked to quinone reduction (Vignais and Billoud, 2007). Mvh hydrogenases

285   are usually associated with heterodisulfide reductases (Hdr) as large complexes

286   (MvhADG/HdrABC), which are proposed to couple the endergonic reduction of ferredoxin with

287   molecular hydrogen to the exergonic reduction of the heterodisulfide with molecular hydrogen by

288   electron bifurcation (Thauer et al., 2008; Thauer et al., 2010). In addition, *mvhADG* genes are

289   sometimes physically located next to *hdr* genes in some sulfate-reducing organisms and can act as

290   electron acceptors in a process that may involve in electron bifurcation (Pereira et al., 2011). In the

291   DR15 genome, *mvhADG* genes were also adjacent to the *hdr* genes (Fig. S6 and Table S1),

292   indicating that the Mvh hydrogenase may perform the same function as in sulfate-reducing

293   bacteria. Ech complexes are widespread in both anaerobic and facultative anaerobic

294   bacteria/archaea and couple the exergonic electron transfer from reduced ferredoxin to H^+ or the

295   reduction of ferredoxin with molecular hydrogen (Schuchmann and Muller, 2014). In the epibiont

296   genome, the gene cluster encoding for Ech complex was present in the same synton than a gene

297 coding for a putative formate dehydrogenase (Table S1). Therefore, the Ech complex is a possible

298 candidate for energy-coupling in the WL pathway of strain DR15 (Fig. S6). This is similar to

299 *Moorella thermoacetica,* in which Ech activity is coupled to the generation of a transmembrane

300 electrochemical H^+ gradient (Schuchmann and Muller, 2014).

301   Transcriptomic analysis revealed that all of these hydrogenase genes were expressed. They

302 were involved either in the oxidation of H_2 coupled to the reduction of sulfate, or in electron

303 transfer and cofactor regeneration. We observed that, at the time of sampling, genes encoding

304 hydrogenases were expressed at significantly lower levels than genes involved in

305 disproportionation of inorganic sulfur compounds (Table S1). Hence, based on the transcriptomic

306 data, at the time of sampling the strain might harvest more energy from sulfur compounds

307 disproportionation than from hydrogen oxidation.

308

309 **Nitrogen metabolism**

310 Based on the genomic data, DR15 has the potential to use ammonia, urea and molecular nitrogen

311 as nitrogen sources, which represents a wider range of nitrogen sources than previously described

312 for campylobacterial and gammaproteobacterial epibionts of *R. exoculata* (Jan et al., 2014). The

313 draft genome contains ammonium permeases (Amt), glutamine synthase (GlnA), and glutamate

314 synthase (GltBD) for ammonia assimilation (Fig. 3 and Table S1). The *glnK* gene encoding a

315 regulatory protein P-II was linked to the *amt* gene for ammonia transport, indicating that the

316 nitrogen metabolism in DR15 could be regulated similarly to *E. coli* (Javelle et al., 2004). In

317 addition, the DR15 genome encodes a urea ABC transporter for urea uptake, as well as a urease

318 operon that is involved in urea hydrolysis, suggesting that DR15 could also utilize urea to generate

319 ammonia, which has not been observed in the campylobacterial and gammaproteobacterial

320 epibionts (Jan et al., 2014). Surprisingly, DR15 was found to potentially be capable of nitrogen

321 fixation. Nearly all of the genes involved in this process were present within the draft genome,

322 including *nifHDK* encoding for a molybdenum-iron nitrogenase, *nifENB, nifU* and *nifS* for

323 assembly proteins, and *nifA* and *ntrXY* for regulator proteins (Table S1). Similarly, in the

324 sulfur-disproportionating deltaproteobacterium *Desulfocapsa sulfexigens*, all of the genes

325 necessary for nitrogen fixation were observed in the genome (Finster et al., 2013). Therefore, it is

326 possible that DR15 can grow by utilizing free nitrogen gas as the sole nitrogen source. Symbiotic

327 nitrogen-fixers are known to be associated with wood-boring bivalves, coral, sponges and sea

328 urchins (Fiore et al., 2010). Recently, Petersen et al. provided the first report of nitrogen fixation

329 by a chemosynthetic symbiont in a shallow water bivalve (Petersen et al., 2016). Nitrogen fixation

330 may be more important in the deep-sea environment, especially as nitrogen sources are scarce.

331 However, prior to this study, nitrogen fixation pathways have not been detected in vent animal

332 symbionts. This study reports nitrogen fixation in a chemosynthetic epibiont of *R. exoculata*. In

333 addition, the presence of one denitrification system, including the periplasmic dissimilatory nitrate

334 reductase (Nap) and the nitrite reductase (Nir), indicated that DR15 might have the potential to

335 reduce nitrate to nitrous oxide by dissimilatory nitrate reduction. This ability was also discovered

336 in a gammaproteobacterial epibiont of *R. exoculata* (Jan et al., 2014).

337 　　Transcriptomic data revealed that almost all of the genes required for nitrogen metabolism

338 that were described above were also expressed in strain DR15 (Fig. 3 and Table S1). Among these,

339 the genes involved in ammonia assimilation, such as *amt*, *glnA*, *gltBD*, and *glnK* showed the

340 highest levels of expression, followed by the *urtA* gene for a urea ABC transporter (Fig.3). In

341 contrast, the genes involved in nitrogen fixation were expressed at relatively low levels. These

342 results indicated that, at the time of sampling, DR15 might utilize ammonia as a main nitrogen

343 source, followed by urea. Moreover, ammonia was assimilated mainly by glutamine synthase

344 (Fig.3). Nitrogen fixation may be active when the environment is depleted in nitrogen sources,

345 such as ammonia and urea.

346

347 **Oxidative stress**

348 The DR15 genome encodes multiple copies of genes involved in defense against oxidative stress,

349 such as the rubrerythrin (Rbr)-rubredoxin (Rbo) oxidoreductase system (Table S1). The system

350 consists of Rbr and Rbo, which have been proposed in *Desulfovibrio vulgaris* as an oxidative

351 stress protection system that is an alternative to superoxide dismutase (SOD) (Lumppio et al.,

352 2001). In addition, the genome also encodes a bd-type cytochrome terminal oxidase (Fig. 3 and

353 Table S1). This enzyme reduces molecular oxygen using electrons from the quinone pool in

354 *Desulfovibrio* species (Cypionka, 2000), thereby protecting cells from molecular oxygen. The

355 presence and expression of the Rbr-Rbo system and of its regulator (PerR), as well as bd-type

356 cytochromes, could indicate that *Candidatus* Desulfobulbus rimicarensis encounters a wide range

357   of redox gradients as the shrimp swims through the vent environment.

358

359   **Amino acid and cofactor biosynthesis**

360   Strain DR15 can synthesize all 20 amino acids, as all the genes essential for amino acid

361   biosynthesis were present in the genome and were expressed (Table S1). DR15 also contains all

362   genes required for the biosynthesis of selenocysteine, an essential catalytic component for the

363   selenium-containing variant of formate dehydrogenase in the WL pathway (Shin et al., 2016). In

364   addition, this bacterium has the genetic potential to synthesize vitamin B12, B1, and B6, as well as

365   many other cofactors. Vitamin B12 is essential for both the methyl and carboxyl branches of the

366   WL pathway. The draft genome contains an almost complete set of the genes required for

367   synthesizing cobalamin *via* precorrin-2 (Table S1). The biosynthesis of biotin, heme and siroheme,

368   riboflavin, folate, and tetrahydrofolate, pantothenate and coenzyme A, NAD and NADP, and a

369   molybdenum cofactor could also be performed in this bacterium, based on the presence of the

370   required genes (Table S1). However, the genes involved in the biosynthesis of menaquinone are

371   incomplete, which suggests that the epibiont might depend on an external supply of this

372   compound or that these genes were not captured due to missing portions of the draft genome. All

373   genes involved in cofactor biosynthesis were expressed, and the genes required for vitamin B6

374   biosynthesis exhibited the highest expression levels.

375

376   **Comparative genomic analyses suggest adaptations to an epibiotic lifestyle.** A

377   comparative whole-genome analysis revealed the likely adaptive features between symbiotic and

378   free-living *Desulfobulbus* species (Pagani et al. 2011; Sass et al. 2002; Suzuki et al. 2007). Genes

379   from three *Desulfobulbus* genomes used in the comparison were subjected to a pan genome

380   analysis. Of these, 930 occurred in both the shrimp-associated and free-living genome pools, and

381   1553 and 537 genes were specific to the shrimp-associated and free-living pool, respectively. As a

382   shrimp epibiont, strain DR15 displayed unique symbiotic features, such as carbon and energy

383   metabolisms (Fig. 4). The prediction of a functional WL pathway for carbon fixation was only

384   present in strain DR15, with an enrichment of CO dehydrogenase/acetyl-CoA synthase (8 genes in

385   epibiotic *vs*. 1-2 genes in free-living genomes). The presence of a functional WL pathway in this

386   epibiont might guarantee a steady carbon supply to the host and ensure its ecological success.

387 Regarding sulfur metabolism, strain DR15 has genes that could potentially reduce tetrathionate

388 and thiosulfate, with six genes encoding for tetrathionate reductase and four genes encoding for

389 thiosulfate reductase, whereas these genes were almost completely absent in the genomes of

390 free-living species. Moreover, seven genes encoding for the uptake of glutamate and aspartate

391 were present in the epibiont genome, whereas only one gene was found in three free-living strains,

392 suggesting that strain DR15 may have a capability to uptake glutamate or aspartate, possibly from

393 the shrimp host, while free-living strains would not have this ability. In addition, strain DR15 also

394 shows an enrichment in CRISPR-associated protein, including Cas, Csd, Csm, and Cmr family

395 proteins (16 genes in strain DR15 *vs*. 2-8 genes in genomes of free-living species) (Fig. 4). The

396 genomic signature is commonly reported as diagnostic of a typical sponge symbiotic life-style

397 (Horn et al., 2016), here it probably hints at a yet unrevealed role of these proteins in

398 shrimp-epibiont interactions.

399 The strain DR15 genome can also be distinguished from the genomes of free-living strains as

400 it lacks genes encoding for several features typically reported in free-living strains. There were no

401 genes coding for flagellum synthesis or chemotaxis proteins in the DR15 genome, whereas around

402 64–82 of genes coding for these features were present in the genomes of free-living species (Fig.4),

403 suggesting a non-motile lifestyle. Genes responsible for the biosynthesis of capsular

404 polysaccharide (CPS) and extracellular polysaccharide (EPS) were almost completely lost in strain

405 DR15 (Fig. 4). CPS and EPS are extracellular polysaccharides common in a wide range of

406 microorganisms that play important roles, such as protection against environmental stresses,

407 biofilm formation, and resistance to phagocytosis or antibiotic treatments. The absence of CPS

408 and EPS suggests that strain DR15 is weakly protected from extracellular stresses, which is

409 compensated by being located inside the cephalothoracic chamber. By contrast, this characteristic

410 is likely to diminish the barrier between the symbiont and shrimp cells, thus benefiting

411 shrimp-epibiont interactions and nutrient exchange. Furthermore, there was also a dramatic

412 reduction in genes involved in resistance to antibiotics and environmental toxins in strain DR15

413 genome (Fig. 4), such as, multidrug resistance efflux and cobalt-zinc-cadmium resistance.

414 Resistance to these toxins in open water is important for the survival of microorganisms; however,

415 strain DR15 could escape these toxins by being sheltered by its shrimp host. In addition, the type I

416 restriction-modification involved in DNA metabolism, as well as the type IV protein and

417 nucleoprotein secretion system involved in membrane transporter, were also dramatically reduced

418 in the epibiont genome.

419

420 **Syntrophic association.** Multiple symbionts have been found to co-occur in both deep-sea and

421 shallow-water hosts, such as mussels, worms, shrimps, and snails (Dubilier et al., 2008; Jan et al.,

422 2014; Ponnudurai et al., 2017). Stable associations between multiple symbionts within a host are

423 assumed to be beneficial to each other (Dubilier et al., 2001; Woyke et al., 2006). Although the

424 co-occurrence of sulfur oxidizers and deltaproteobacterial epibionts raises the possibility of an

425 internal sulfur cycle that would take place within the shrimp cephalothoracic chamber (Hugler et

426 al., 2011), this hypothesis is solely based on 16S rRNA gene sequencing and functional gene

427 surveys. This study probably supports the existence of a syntrophic relationship between

428 sulfur-disproportionating *Deltaproteobacteria*, and sulfur-oxidizing bacteria, including

429 *Campylobacteria* and *Gammaproteobacteria*, which are associated with *R. exoculata* (Fig. 5).

430 Considering that species of *Campylobacteria* and *Gammaproteobacteri*a are filamentous in shape

431 (Petersen et al., 2010; Hugler et al., 2011; Guri et al., 2012), these bacterium anchor to the surface

432 of the scaphognathite setae at one end of the cell and use the other end to scavenge sulfide

433 compounds from the interior of the cephalothoracic chamber, producing partially oxidized

434 inorganic sulfur compounds (POSCs) *via* sulfide oxidation. In contrast, deltaproteobacterial

435 epibionts settle close to the surface of the scaphognathite setae, as observed by Hugler et al.

436 (Hugler et al., 2011). These bacteria seem to be able to utilize the POSCs that are either 1)

437 produced by *Campylobacteria* and *Gammaproteobacteria* or 2) directly transferred from the

438 surrounding environments for disproportionation. In return, the sulfide derived from

439 disproportionation could come back to the *Campylobacteria* and *Gammaproteobacteria* for

440 reoxidation (Fig. 5). Thus, if this hypothesis was confirmed, these different epibiotic styles would

441 not compete for energy sources, but rather share a mutualistic relationship with each other in an

442 epibiotic sulfur cycle. These bacterial species could be specialized to fit into micro-niches and

443 build a harmonious relationship with their host. Deltaproteobacterial epibionts would tend to

444 reside in the anoxic or oxic-anoxic interfaces on the close surface of the scaphognathite setae,

445 while *Campylobacteria* and *Gammaproteobacteria* thrive in the oxic zone, on the scaphognathite

446 setae of *R. exoculata*. This syntrophic association would be based on the exchange of reduced and

447   oxidized sulfur compounds, as already described for an oligochaete worm (Dubilier et al., 2001).

448

449   **Description of *Candidatus* Desulfobulbus rimicarensis**

450   *Candidatus* Desulfobulbus rimicarensis (ri.mi'ca'ren'sis. L. fem. adj. rimicarensis, referring to

451   *Rimicaris exoculata*, the host shrimp where the species was found. Desulfobulbus rimicarensis, a

452   *Rimicaris exoculata* epibiont).

453   **Properties**: Phylogenetic analysis shows that the novel strain belongs to the genus *Desulfobulbus*,

454   but forms a separate cluster with other members of this genus. The cell colonizes the surface of

455   scaphognathite setae in the cephalothoracic chamber of *R. exoculata*, a shrimp inhabiting deep-sea

456   hydrothermal vents from the Atlantic Ocean. The bacterium was likely to grow

457   chemolithoautotrophically by disproportionation of inorganic sulfur compounds, or molecular

458   hydrogen oxidation coupled to sulfate reduction, under reduced conditions. It has the genetic

459   potential to utilize diverse nitrogen sources, including ammonia, urea, and free nitrogen gas.

460   **Metabolic activity**: In its natural environment, this bacterium is likely to utilize carbon dioxide as

461   the main carbon source. Growth might be supported by the disproportionation of reduced sulfur

462   compounds. Ammonia and urea might be used as nitrogen sources. The metabolic plasticity and

463   activity of this deltaproteobacterial epibiont of a shrimp is likely to confer an adaptive advantage

464   to the shrimp in the highly dynamic hydrothermal mixing zone.

465

466   # CONCLUSION

467   Although *Deltaproteobacteria* are ubiquitous in epibiotic communities of *R. exoculata* in deep-sea

468   hydrothermal vent environments (Hugler et al., 2011; Guri et al., 2012; Jan et al., 2014), their

469   ecological function and symbiotic adaptation to the shrimp host are not clear. In this report, we

470   described a novel bacterium *Candidatus* Desulfobulbus rimicarensis*, which represents a

471   characterized (while still uncultivated) deltaproteobacterial epibiont of this deep-sea hydrothermal

472   vent shrimp. Compared to other epibionts that inhabit the cephalothoracic chamber of *R. exoculata*

473   (Jan et al., 2014), this bacterium possesses unique metabolic pathways, such as the WL pathway,

474   sulfur disproportionation (potentially also sulfate reduction), and nitrogen fixation pathways. We

475   hypothesize that this bacterium is involved in a syntrophic association with the sulfur-oxidizing

476 campylobacterial and gammaproteobacterial epibionts of the cephalothoracic chamber through the

477 exchange of sulfur compounds of differing redox levels. In addition, the genome of this epibiont

478 could be distinguished from its free-living counterparts by its reduced genome size, the lack of

479 chemotaxis and motility traits, dramatic reduction of genes involved in the biosynthesis of CPS

480 and EPS, lack of resistance towards environmental toxins, and enrichment of genes required for

481 the carbon fixation and sulfur metabolism. These genetic modifications suggest that *Candidatus*

482 Desulfobulbus rimicarensis is adapted to its shrimp host.

483

MATERIALS AND METHODS

Shrimp collection and nucleic acid extraction. Vent shrimps were collected using a grabber during the DY115-26 oceanographic cruise leg III on the South MAR (Site SMAR-S029-TVG11, 15.17°S, 13.36°W, 2807 m depth) (Supporting Information Fig. S1), with Zongze Shao as the chief scientist. Phylogenetic analysis of the mitochondrial cytochrome oxidase subunit I (COI) genes (Dong et al. 2019) showed that they were most closely related to species *Rimicaris exoculata*, which was firstly found in the north Mid-Atlantic Ridge (Williams and Rona, 1986). Once aboard, *R. exoculata* specimens were immediately stored in liquid nitrogen and frozen at −80°C for DNA and RNA extractions. In the laboratory, four specimens were dissected under sterile conditions and the mouthparts were immediately used to extract DNA and RNA. DNA was extracted using a modification of SDS-based DNA extraction method (Zhou et al., 1996). Samples were mixed with 13.5 ml DNA extraction buffer, vortexed vigorously for 1 minute and incubated in an orbital shaker at 37℃ for 30 min. Then 1.5 ml 20 % SDS was added and the samples were incubated in a shaking water bath at 65℃ for 1 h, After centrifugation at 6,000g for 20 min, DNA supernatant was precipitated with phenol, chloroform, and isopropanol. RNA was extracted using a TRI REAGENT procedure (Chomczynski, 1993). After each extraction, DNA and RNA were assessed with a NanoDrop system (Thermo NanoDrop™ 2000, Wilmington, Delaware, USA) and the gel electrophoresis to determine concentration and integrity, and then were sent to the Chinese National Human Genome Center in Shanghai for high throughput sequencing.

Assembly, binning and annotation of individual genome. Metagenomic DNA sequencing was performed with an Illumina MiSeq platform (500-bp library) at the National Human Genome Centre of China at Shanghai, China, according to the manufacturer's manual. This produced a total of 14,553,576 reads with a total length of 8.7Gbp. All these reads were imported into CLC Genomics Workbench 6.5 (http://www.clcbio.com) and trimmed using a quality score of 0.01 and a minimum length of 50 bp. Subsequently, the trimmed reads were assembled with the following modified parameters: wordsize, 61; bubble size, 200; minimum contig length of 200 bp. This procedure resulted in 1,030,504 contigs (11,026 contigs ≥ 1000 bp)

with a total length of 394,265,091 bp. The contig coverage was calculated by mapping the trimmed reads to reference algorithm using the minimum similarity of 95% of the read length. Binning of the draft genomes was carried out based on tetranucleotide frequency by utilizing Databionics ESOM-map software (Ultsch, 2005) with the same parameters as described by Dick et al. (Dick et al., 2009). Final results were manually curated for species assignment of contigs based on their coverage, GC content and blast results against nr database. Contigs with ambiguous taxonomic assignments were discarded for the rest of the analysis. Purity and completeness of genome bins were then assessed by CheckM v.1.0.7 (Parks et al., 2015) using the lineage-specific workflow. Open reading frames (ORFs) were identified using Prodigal (version 2.6.3) (Hyatt et al., 2010). The conserved single-copy gene (CSCG) of genome bins were identified by searching identified amino acid sequences against a HMM database of 107 universally prokaryotic genes (Albertsen et al., 2013) using hmmsearch with default settings.

Gene annotation of the resulting draft genome was performed by Rapid Annotation using Subsystem Technology (RAST) server (Aziz et al., 2008) and the NCBI Prokaryotic Genomes Automatic Annotation Pipeline (PGAAP). Metabolic reconstruction of DR15 was performed based on a list of functional genes involved in important metabolic pathways (Supporting Information Table S2), each of which was automatically and then manually curated by comparing the predicted protein sequences with those in GenBank databases. In addition, the CRISPR-Cas system of strain DR15 was searched using the CRISPRCasFinder (https://crisprcas.i2bc.paris-saclay.fr/CrisprCasFinder/Index). The webserver HydDB (https://services.birc.au.dk/hyddb/) was used for the hydrogenase classification (Søndergaard et al., 2016).

Metatranscriptomic analyses. The extracted RNA was treated with DNase I (Takara, Japan) to remove genomic DNA. Ribosomal RNA (rRNA) was removed from the total RNA using the Ribo-Zero™ Magnetic Kit (Epicentre, USA). A total of 100 ng rRNA-depleted RNA was used for cDNA library preparation. Sequencing libraries were constructed by NEBNext® Ultra™ Directional RNA Library Prep Kit for Illumina (NEB, USA) following the manufacturer's protocol. The cDNA was directly sequenced using the Illumina HiseqTM^{2500} platform at the National Human Genome Centre of China at Shanghai, China. The obtained raw $2\times$ 100-bp

paired-end reads were subjected to quality control using the next-generation sequencing (NGS) FASTX-Toolkit (http://hannonlab.cshl.edu/fastx_toolkit/) with a quality score of 0.01 and a minimum length of 50 bp, resulting a total of 5.38 Gbp clean data. To depict the gene expression profiling for each genomic bin, the dereplicated, trimmed, and paired-end Illumina reads were then mapped to contigs from the DR15 genome using Bowtie, version 1.1.1 (http://bowtie-bio.sourceforge.net/index.shtml),with parameters specifically chosen for RNA-Seq quantification (-n 2, -e 99999999, -l 25) (Langmead and Salzberg, 2012). FPKM (fragments per kilobase of transcript per million fragments mapped) was used to estimate the expression level of each gene using RSEM-1.2.3（http://deweylab.biostat.wisc.edu/rsem/）with the default parameters.

Phylogenetic analysis. In order to elucidate the taxonomic positions of *Candidatus* Desulfobulbus rimicarensis, the bacterial core gene-based phylogenetic analysis was carried out using the Up-to-date Bacterial Core Gene pipeline (UBCG) (Na et al., 2018). The whole genome sequences of reference taxa were obtained from NCBI database. The 92 concatenated gene sequences were extracted, aligned and concatenated within UBCG using default parameters. A maximum-likelihood phylogenetic tree was inferred using RAxML version 8.2.11 (Stamatakis, 2014) with the GTR+CAT model and 100 bootstrap replications.

Comparative genomics. Comparative genome analysis was performed using the Bacterial Pan Genome Analysis pipeline (BPGA) (Chaudhari et al., 2016). Core genes were detected using the USEARCH program (v. 11.0) (Edgar et al., 2010) extracted from the whole genome sequences of the four strains, with a 50% sequence identity cut-off. The pan genome analysis also complied a set of accessory genes present in at least two or more strains, and unique genes only found in a single strain.

Fluorescence in situ hybridization. The FISH protocol was modified based on a previous description Petersen et al. (Petersen et al., 2010). Whole scaphognathite tissues were embedded in the Tissue Freezing Medium (Leica, Germany) and 5μm thick sections cut with a CM 1850 microtome (Leica, Germany). The sections were collected on Adhesion Microscope slides (Citotest, China). Sections were hybridized in a buffer (0.9 M NaCl, 0.02 M Tris/HCl pH 8.0, 0.01%

573 SDS, 35% formamide) containing probes at an end concentration of 5 ng μl^{-1} for 3 h at 46°C, then

574 washed for 30 min at 48°C with washing buffer (0.08 M NaCl, 0.02 M Tris/HCl pH 8.0, 0.01%

575 SDS, 5 mm EDTA), then dipped briefly in MQ water and 96 % ethanol, then air dried. To stain all

576 DNA, sections were covered with 10 μl of a 1 μg ml^{-1} DAPI solution and incubated for 3-10

577 minutes, then rinsed with MQ water and 96 % ethanol, then air dried. Branchiostegite sections

578 were hybridized using probes Eub338 (Amann et al., 1990) and DSB706 (Manz W, 1992).

579 Observations and imaging were performed using both a fluorescence microscope (Leica

580 DM6000B, Germany) and a confocal laser-scanning microscope (Leica TCS SP5, Germany).

581

582 **Nucleotide sequence accession number.** Metagenomic and Metatranscriptomic data were

583 submitted to the Sequence Read Archive (SRA) database of NCBI under accession numbers

584 SRX4896442 and SRX4896443, respectively. The draft genome of *Candidatus* 'Desulfobulbus

585 rimicarensis' was deposited at DDBJ/ENA/GenBank under the accession RKSL00000000. The

586 version described in this paper is version RKSL01000000.

587

ACKNOWLEDGEMENTS

593

CONFLICT OF INTEREST

595 The author declare no conflict of interest.

REFERENCES

1. Albertsen M, Hugenholtz P, Skarshewski A, Nielsen KL, Tyson GW, Nielsen PH. 2013. Genome sequences of rare, uncultured bacteria obtained by differential coverage binning of multiple metagenomes. Nat Biotechnol 31: 533-538.

2. Amann RI, Krumholz L, Stahl DA. 1990. Fluorescent-oligonucleotide probing of whole cells for determinative, phylogenetic, and environmental studies in microbiology. J Bacteriol 172: 762-770.

3. Aziz RK, Bartels D, Best AA, DeJongh M, Disz T, Edwards RA et al. 2008. The RAST Server: rapid annotations using subsystems technology. BMC Genomics 9: 75.

4. Bak F, Pfennig N. 1987. Chemolithotrophic growth of *Desulfovibrio sulfodismutans* sp. nov. by disproportionation of inorganic sulfur compounds. Arch. Microbiol. 147:184-189.

5. Beinart RA, Gartman A, Sanders JG, Luther GW, Girguis PR. 2015. The uptake and excretion of partially oxidized sulfur expands the repertoire of energy resources metabolized by hydrothermal vent symbioses. Proc Biol Sci 282: 20142811.

6. Chaudhari NM, Gupta VK, Dutta C. 2016. BPGA-an ultra-fast pan-genome analysis pipeline. Scientific reports 6: 24373.

7. Chomczynski P. 1993. A reagent for the single-step simultaneous isolation of RNA, DNA and proteins from cell and tissue samples. Biotechniques 15: 532-534, 536-537.

8. Cohen SS. 1998. A Guide to the Polyamines. Oxford University Press, New York.

9. Cypionka H. 2000. Oxygen respiration by *Desulfovibrio* species. Annu Rev Microbiol 54: 827-848.

10. Cypionka MKaH. 1989. Sulfate formation via ATP sulfurylase in thiosulfate- and sulfite-disproportionating bacteria. Arch Microbiol 151: 232- 237.

11. De Cian M, Regnault M, Lallier FH. 2000. Nitrogen metabolites and related enzymatic activities in the body fluids and tissues of the hydrothermal vent tubeworm Riftia pachyptila. J Exp Biol 203: 2907-2920.

12. Dick GJ, Andersson AF, Baker BJ, Simmons SL, Thomas BC, Yelton AP, Banfield JF. 2009. Community-wide analysis of microbial genome sequence signatures. Genome Biol 10: R85.

13. Dong CM, Xie YR, Li HM, Lai QL, Liu XP, Shao ZZ. 2009. Faunal and microbial biodiversity of the newly discovered Deyin-1 hydrothermal vent field at 15°S on the southern Mid-Atlantic Ridge. Deep-Sea Research Part I: Oceanographic Research Papers 153:103134.

14. Dubilier N, Bergin C, Lott C. 2008. Symbiotic diversity in marine animals: the art of harnessing chemosynthesis. Nat Rev Microbiol 6: 725-740.

15. Dubilier N, Mulders C, Ferdelman T, de Beer D, Pernthaler A, Klein M et al. 2001. Endosymbiotic sulphate-reducing and sulphide-oxidizing bacteria in an oligochaete worm. Nature 411: 298-302.

16. Edgar RC. 2010. Search and clustering orders of magnitude faster than BLAST. Bioinformatics 26: 2460-2461.

17. Finster K, Liesack W, Thamdrup B. 1998. Elemental sulfur and thiosulfate disproportionation by *Desulfocapsa sulfoexigens* sp. nov., a new anaerobic bacterium isolated from marine surface sediment. Appl Environ Microbiol 64: 119-125.

18. Finster K. 2008. Microbiological disproportionation of inorganic sulfur compounds. Journal of Sulfur Chemistry 29: 281-292.

639   19.   Finster KW, Kjeldsen KU, Kube M, Reinhardt R, Mussmann M, Amann R, Schreiber L. 2013.
640   Complete genome sequence of *Desulfocapsa sulfexigens*, a marine deltaproteobacterium
641   specialized in disproportionating inorganic sulfur compounds. Stand Genomic Sci 8: 58-68.

642   20.   Fiore CL, Jarett JK, Olson ND, Lesser MP. 2010. Nitrogen fixation and nitrogen
643   transformations in marine symbioses. Trends Microbiol 18: 455-463.

644   21.   Frederiksen TM, Finster K. 2004. The transformation of inorganic sulfur compounds and the
645   assimilation of organic and inorganic carbon by the sulfur disproportionating bacterium
646   *Desulfocapsa sulfoexigens*. Antonie Van Leeuwenhoek 85: 141-149.

647   22.   Garman A, Yucel M, Madison SA, Chu DW, Ma SF, Janzen CP et al. 2011. Sulfide oxidation
648   across diffuse flow zones of hydrothermal vents. Aquat Geochem 17: 583-601.

649   23.   Gebruk AV, Southward EC, Kennedy H, Southward AJ. 2000. Food sources, behaviour, and
650   distribution of hydrothermal vent shrimps at the Mid-Atlantic Ridge. J Mar Biol Assoc U K
651   80: 485-499.

652   24.   Grein F, Pereira IA, Dahl C. 2010. Biochemical characterization of individual components of
653   the Allochromatium vinosum DsrMKJOP transmembrane complex aids understanding of
654   complex function in vivo. J Bacteriol 192: 6369-6377.

655   25.   Gru C, Sarradin PM, Legoff H, Narcon S, Caprais JC, Lallier FH. 1998. Determination of
656   reduced sulfur compounds by high-performance liquid chromatography in hydrothermal
657   seawater and body fluids from Riftia pachyptila. Analyst 123: 1289-1293.

658   26.   Guenther BD, Sheppard CA, Tran P, Rozen R, Matthews RG, Ludwig ML. 1999. The
659   structure and properties of methylenetetrahydrofolate reductase from *Escherichia coli*
660   suggest how folate ameliorates human hyperhomocysteinemia. Nat Struct Biol 6: 359-365.

661   27.   Guri M, Durand L, Cueff-Gauchard V, Zbinden M, Crassous P, Shillito B, Cambon-Bonavita
662   MA. 2012. Acquisition of epibiotic bacteria along the life cycle of the hydrothermal shrimp
663   *Rimicaris exoculata*. ISME J 6: 597-609.

664   28.   Horn H, Slaby BM, Jahn MT *et al.* 2016. An enrichment of CRISPR and other
665   defense-related features in marine sponge-associated microbial metagenomes. Front
666   Microbiol 7: 1751.

667   29.   Hugler M, Sievert SM. 2011. Beyond the Calvin cycle: autotrophic carbon fixation in the
668   ocean. Ann Rev Mar Sci 3: 261-289.

669   30.   Hugler M, Petersen JM, Dubilier N, Imhoff JF, Sievert SM. 2011. Pathways of carbon and
670   energy metabolism of the epibiotic community associated with the deep-sea hydrothermal
671   vent shrimp *Rimicaris exoculata*. PLoS One 6: e16018.

672   31.   Hyatt D, Chen GL, Locascio PF, Land ML, Larimer FW, Hauser LJ. 2010. Prodigal:
673   prokaryotic gene recognition and translation initiation site identification. BMC
674   Bioinformatics 11: 119.

675   32.   Igari S, Ohtaki A, Yamanaka Y, Sato Y, Yohda M, Odaka M et al. 2011. Properties and crystal
676   structure of methylenetetrahydrofolate reductase from *Thermus thermophilus* HB8. PLoS
677   One 6: e23716.

678   33.   Jackson BE, McInerney MJ. 2000. Thiosulfate disproportionation by *Desulfotomaculum*
679   *thermobenzoicum*. Appl Environ Microbiol. 66:3650-3.

680   34.   Jan C, Petersen JM, Werner J, Teeling H, Huang S, Glockner FO et al. 2014. The gill
681   chamber epibiosis of deep-sea shrimp *Rimicaris exoculata*: an in-depth metagenomic
682   investigation and discovery of Zetaproteobacteria. Environ Microbiol 16: 2723-2738.

683 35. Javelle A, Severi E, Thornton J, Merrick M. 2004. Ammonium sensing in *Escherichia coli*.
684   Role of the ammonium transporter AmtB and AmtB-GlnK complex formation. J Biol Chem
685   279: 8530-8538.

686 36. Kojima H, Umezawa K, Fukui M. 2016. *Caldimicrobium thiodismutans* sp. nov., a
687   sulfur-disproportionating bacterium isolated from a hot spring, and emended description of
688   the genus *Caldimicrobium*. Int J Syst Evol Microbiol. 66:1828-31

689 37. Kumar S, Stecher G, Tamura K. 2016. MEGA7: Molecular Evolutionary Genetics Analysis
690   Version 7.0 for Bigger Datasets. Mol Biol Evol 33: 1870-1874.

691 38. Kumari S, Tishel R, Eisenbach M, Wolfe AJ. 1995. Cloning, characterization, and functional
692   expression of acs, the gene which encodes acetyl coenzyme A synthetase in *Escherichia coli*.
693   J Bacteriol 177: 2878-2886.

694 39. Langmead B, Salzberg SL. 2012. Fast gapped-read alignment with Bowtie 2. Nat Methods 9:
695   357-359.

696 40. Lovley DR, Phillips EJ. 1994. Novel processes for anaerobic sulfate production from
697   elemental sulfur by sulfate-reducing bacteria. Appl Environ Microbiol 60: 2394-2399.

698 41. Lumppio HL, Shenvi NV, Summers AO, Voordouw G, Kurtz DM, Jr. 2001. Rubrerythrin and
699   rubredoxin oxidoreductase in *Desulfovibrio vulgaris*: a novel oxidative stress protection
700   system. J Bacteriol 183: 101-108.

701 42. Manz W, AR, Ludwig W, Wagner M, Schleifer KH. 1992. Phylogenetic oligodeoxynucleotide
702   probes for the major subclasses of proteobacteria - problems and solutions. Syst Appl
703   Microbiol 15: 593–600.

704 43. Mullaugh KM, Luther GW, Ma SF, Moore TS et al. 2008. Voltammetic (micro)electrodes for the
705   in situ study of Fe^{2+} oxidation kinetics in hot springs and $S_2O_3^{2-}$ production at hydrothermal vents.
706   Electroanalysis 20: 280-290.

707 44. Na SI, Kim YO, Yoon SH, Ha SM, Baek I, Chun J. 2018.. UBCG: Up-to-date bacterial core
708   gene set and pipeline for phylogenomic tree reconstruction. *J. Microbiol.* 56: 281–285.

709 45. Obraztsova AY, Francis CA, Tebo BM. 2002. Sulfur disproportionation by the facultative
710   anaerobe *Pantoea agglomerans* as a mechanism for chromium (VI) reduction. Geomicrobiol.
711   J. 19: 121-132.

712 46. Oliveira TF, Vonrhein C, Matias PM, Venceslau SS, Pereira IA, Archer M. 2008. The crystal
713   structure of *Desulfovibrio vulgaris* dissimilatory sulfite reductase bound to DsrC provides
714   novel insights into the mechanism of sulfate respiration. J Biol Chem 283: 34141-34149.

715 47. Ollivier B, Zeyen N, Gales G, Hickman-Lewis K, Gaboyer F, Benzerara K, Westall F.   2018.
716   Importance of Prokaryotes in the Functioning and Evolution of the Present and Past Geosphere
717   and Biosphere. In *Prokaryotes and Evolution*; Jean-Claude Bertrand, Philippe Normand, Bernard
718   Ollivier, Télesphore Sime-Ngando (Editors), Springer Nature Switzerland, pp. 68-75.

719 48. Pagani I, Lapidus A, Nolan M et al. 2011. Complete genome sequence of *Desulfobulbus*
720   *propionicus* type strain (1pr3). Stand Genomic Sci 4 (1), 100-110.

721 49. Parks DH, Imelfort M, Skennerton CT, Hugenholtz P, Tyson GW. 2015. CheckM: assessing
722   the quality of microbial genomes recovered from isolates, single cells, and metagenomes.
723   Genome Res 25: 1043-1055.

724 50. Pereira IA, Ramos AR, Grein F, Marques MC, da Silva SM, Venceslau SS. 2011. A
725   comparative genomic analysis of energy metabolism in sulfate reducing bacteria and archaea.
726   Front Microbiol 2: 69.

727 51. Pereira IAC. 2008. "Membrane complexes in *Desulfovibrio*," in Microbial Sulfur Metabolism,
728   eds C. Friedrich and C. Dahl (Berlin: Springer-Verlag). 24-35.

729 52. Petersen JM, Ramette A, Lott C, Cambon-Bonavita MA, Zbinden M, Dubilier N. 2010. Dual
730   symbiosis of the vent shrimp *Rimicaris exoculata* with filamentous gamma- and
731   epsilonproteobacteria at four Mid-Atlantic Ridge hydrothermal vent fields. Environ
732   Microbiol 12: 2204-2218.

733 53. Petersen JM, Kemper A, Gruber-Vodicka H, Cardini U, van der Geest M, Kleiner M et al.
734   2016. Chemosynthetic symbionts of marine invertebrate animals are capable of nitrogen
735   fixation. Nat Microbiol 2: 16195.

736 54. Pierce E, Xie G, Barabote RD, Saunders E, Han CS, Detter JC et al. 2008. The complete
737   genome sequence of *Moorella thermoacetica* (f. *Clostridium thermoaceticum*). Environ
738   Microbiol 10: 2550-2573.

739 55. Pires RH, Lourenco AI, Morais F, Teixeira M, Xavier AV, Saraiva LM, Pereira IA. 2003. A
740   novel membrane-bound respiratory complex from *Desulfovibrio desulfuricans* ATCC 27774.
741   Biochim Biophys Acta 1605: 67-82.

742 56. Polz MF, Cavanaugh CM. 1995. Dominance of one bacterial phylotype at a Mid-Atlantic
743   Ridge hydrothermal vent site. Proc Natl Acad Sci U S A 92: 7232-7236.

744 57. Ponnudurai R, Kleiner M, Sayavedra L, Petersen JM, Moche M, Otto A et al. 2017.
745   Metabolic and physiological interdependencies in the *Bathymodiolus azoricus* symbiosis.
746   ISME J 11: 463-477.

747 58. Ponsard J, Cambon-Bonavita MA, Zbinden M, Lepoint G, Joassin A, Corbari L et al. 2013.
748   Inorganic carbon fixation by chemosynthetic ectosymbionts and nutritional transfers to the
749   hydrothermal vent host-shrimp *Rimicaris exoculata*. ISME J 7: 96-109.

750 59. Richter M, Rossello-Mora R. 2009. Shifting the genomic gold standard for the prokaryotic
751   species definition. Proc Natl Acad Sci U S A 106: 19126-19131.

752 60. Rieley G, Van Dover CL, Hedrick DB, Eglinton G. 1999. Trophic ecology of *Rimicaris
753   exoculata*: a combined lipid abundance stable isotope approach. Mar Biol 133: 495-499.

754 61. Sass A, Rütters H, Cypionka H, Sass H. 2002. *Desulfobulbus mediterraneus* sp. nov., a
755   sulfate-reducing bacterium growing on mono- and disaccharides. Arch Microbiol.
756   177:468-74.

757 62. Schmidt C, LBN, Gaill F. 2008. Interactions of deep-sea vent invertebrates with their
758   environment: the case of *Rimicaris exoculata*. J Shellfish Res 27: 79–90.

759 63. Schuchmann K, Muller V. 2014. Autotrophy at the thermodynamic limit of life: a model for
760   energy conservation in acetogenic bacteria. Nat Rev Microbiol 12: 809-821.

761 64. Shin J, Song Y, Jeong Y, Cho BK. 2016. Analysis of the Core Genome and Pan-Genome of
762   Autotrophic Acetogenic Bacteria. Front Microbiol 7: 1531.

763 65. Starai VJ, Escalante-Semerena JC. 2004. Acetyl-coenzyme A synthetase (AMP forming). Cell
764   Mol Life Sci 61: 2020-2030.

765 66. Slobodkin AI, Reysenbach AL, Slobodkina GB, Baslerov RV, Kostrikina NA, Wagner ID,
766   Bonch-Osmolovskaya EA. 2012. *Thermosulfurimonas dismutans* gen. nov., sp. nov., an
767   extremely thermophilic sulfur-disproportionating bacterium from a deep-sea hydrothermal
768   vent. Int J Syst Evol Microbiol. 62:2565-71.

769 67. Slobodkin AI, Reysenbach AL, Slobodkina GB, Kolganova TV, Kostrikina NA,
770   Bonch-Osmolovskaya EA. 2013. *Dissulfuribacter thermophilus* gen. nov., sp. nov., a

771 thermophilic, autotrophic, sulfur-disproportionating, deeply branching deltaproteobacterium
772 from a deep-sea hydrothermal vent. Int J Syst Evol Microbiol 63: 1967–1971.

68. Slobodkin AI, Slobodkina GB, Panteleeva AN, Chernyh NA, Novikov AA, Bonch-Osmolovskaya EA. 2016. *Dissulfurimicrobium hydrothermale* gen. nov., sp. nov., a thermophilic, autotrophic, sulfur-disproportionating deltaproteobacterium isolated from a hydrothermal pond. Int J Syst Evol Microbiol 66: 1022–1026.

69. Slobodkina GB, Kolganova TV, Kopitsyn DS, Viryasov MB, Bonch-Osmolovskaya EA, Slobodkin AI. 2016. *Dissulfurirhabdus thermomarina* gen. nov., sp. nov., a thermophilic, autotrophic, sulfite-reducing and disproportionating deltaproteobacterium isolated from a shallow-sea hydrothermal vent. Int J Syst Evol Microbiol 66: 2515–2519.

70. Søndergaard D, Pedersen CNS, Greening C. 2016 HydDB: A web tool for hydrogenase classification and analysis. Sci Rep 6:34212.

71. Stamatakis A. 2014. RAxML version 8: a tool for phylogenetic analysis and post-analysis of large phylogenies. *Bioinformatics* 30: 1312–1313.

72. Suzuki D, Ueki A, Amaishi A, Ueki K. 2007. *Desulfobulbus japonicas* sp. nov., a novel Gram-negative propionate-oxidizing, sulfate-reducing bacterium isolated from an estuarine sediment in Japan. Int J Syst Evol Microbiol 57:849-855.

73. Thauer RK, Kaster AK, Seedorf H, Buckel W, Hedderich R. 2008. Methanogenic archaea: ecologically relevant differences in energy conservation. Nat Rev Microbiol 6: 579-591.

74. Thauer RK, Kaster AK, Goenrich M, Schick M, Hiromoto T, Shima S. 2010. Hydrogenases from methanogenic archaea, nickel, a novel cofactor, and H_2 storage. Annu Rev Biochem 79: 507-536.

75. Ultsch A, Moerchen F. 2005. "ESOM-Maps: tools for clustering, visualization, and classification with EmergentSOM," in Technical Report Department of Mathematics and Computer Science, University Marburg, Germany, No. 46.

76. Van Dover CL, Fry B, Grassle JF, Humphris S, Rona PA. 1988. Feeding biology of the shrimp *Rimicaris exoculata* at hydrothermal vents on the Mid-Atlantic Ridge. Mar Biol 98: 209-216.

77. Venceslau SS, Lino RR, Pereira IA. 2010. The Qrc membrane complex, related to the alternative complex III, is a menaquinone reductase involved in sulfate respiration. J Biol Chem 285: 22774-22783.

78. Vignais PM, Billoud B. 2007. Occurrence, classification, and biological function of hydrogenases: an overview. Chem Rev 107: 4206-4272.

79. Waite TJ, Moore TS, childress JJ, HSU-KIM H, Mullaugh KM, Nuzzio DB et al. 2008. Variation in sulfur speciation with shellfish presence at a Lau Basin diffuse flow vent site. J Shellfish Res 27: 163-168.

80. Williams AB, Rona PA. 1986. Two New Caridean Shrimps (Bresiliidae) From a Hydrothermal Field on the Mid-Atlantic Ridge. Journal of Crustacean Biology 6: 446-462.

81. Woyke T, Teeling H, Ivanova NN, Huntemann M, Richter M, Gloeckner FO et al. 2006. Symbiosis insights through metagenomic analysis of a microbial consortium. Nature 443: 950-955.

82. Wright PA. 1995. Nitrogen excretion: three end products, many physiological roles. J Exp Biol 198: 273-281.

83. Zbinden M, Le Bris N, Gaill F, Compe`re P. 2004. Distribution of bacteria and associated

815 minerals in the gill chamber of the vent shrimp *Rimicaris exoculata* and related
816 biogeochemical processes. Mar Ecol Prog Ser 284: 237–251.

817 84. Zbinden M, Shillito B, N, LB, De Villardi de Montlaur C, Roussel E, Guyot F. 2008. New
818 insights on the metabolic diversity among the epibiotic microbial communitiy of the
819 hydrothermal shrimp *Rimicaris exoculata*. J Exp Mar Biol Ecol 359: 131–140.

820 85. Zhou J, Bruns MA, Tiedje JM. 1996. DNA recovery from soils of diverse composition. Appl
821 Environ Microbiol 62: 316-322.

FIGURE AND TABLE LEGENDS

Figure 1. The 2.92-Mbp genome and transcriptome of *Candidatus* Desulfobulbus rimicarensis. The outermost ring shows the annotations of the 11 most abundant transcripts in the transcriptome. The second ring (histogram) shows the relative abundance of transcripts based on FPKM (fragments per kilobase of transcript per million fragments mapped). The third and fourth rings (green and red) indicate predicted ORFs on the plus and minus strands, respectively. The fifth ring indicates the location of rRNA and tRNA genes. The sixth and innermost ring display the GC content and GC skew, respectively. Key to transcripts annotations: 1. Adenylylsulfate reductase (AprAB); 2. ATP synthase (AtpABCDEFFG); 3. Sulfatase-modifying factor enzyme 1 (YfmG); 4. Sulfate adenylyltransferase (Sat); 5. Porin-hypothetical protein; 6. Heterodisulfide reductase (QmoABC); 7. Permease (Sulfite exporter TauE/SafE); 8. TusA-related sulfurtransferase; 9. Dissimilatory sulfite reductase *(*DsrABCD); 10. NADH-ubiquinone oxidoreductase (NuoABCDHIJKLM); 11. Thiosulfate reductase (PhsAB). The FRPM of all genes in the draft genome of '*Candidatus* Desulfobulbus rimicarensis' is provided as an SI (Table S1).

Figure 2. A The transcripts abundances of encoding key genes involved in the disproportionation of inorganic sulfur compounds in *Candidatus* Desulfobulbus rimicarensis. **B** Disproportionation of inorganic sulfur compounds and energy conservation in *Candidatus* Desulfobulbus rimicarensis. Transcript abundance is normalized for gene length and total number of reads per dataset (FPKM). Abbreviations: AprAB, adenylylsulfate reductase; Sat, sulfuradenylyltransferase; DsrABCD, reverse-type dissimilatory sulfite reductase; PhsAB, thiosulfate reductase; DsrMKJOP, sulfite reduction-associated complex; QmoABC, putative quinone-interacting membrane-bound oxidoreductase; SUL, sulfate permease; APS, adenylyl sulfate.

Figure 3. Metabolic map reconstructed from the draft genome of *Candidatus* Desulfobulbus rimicarensis. Biosynthetic amino acids, and central vitamin and cofactors are indicated in red on a pink background. Gene transcripts highly expressed are emphasized in purple, and genes with moderate transcript abundances are indicated in orange. Abbreviations: G1P, glucose 1-phosphate; G6P, glucose 6-phosphate; PRPP, phosphoribosyl pyrophosphate; PEP, phosphoenolpyruvate; PG, phosphoglycerate; Ala, alanine; Arg, arginine; Asn, asparagine; Asp, aspartate; Gln, glutamine; Glu, glutamate; Gly, glycine; Ile, isoleucine; Leu, leucine; Lys, lysine; Phe, phenylalanine; Pro, proline; Ser, serine; Thr, threonine; Trp, tryptophan; Tyr, tyrosine; Val, valine; His, *his*tidine; Met, methionine; Cys, *cys*teine; Cah, carbonic anhydrase; PorA, pyruvate-flavodoxin oxidoreductase; PpsA, phosphoenolpyruvate synthase; Tal, transaldolase; Eno, enolase; GapA, glyceraldehyde-3-phosphate dehydrogenase; PycA, pyruvate carboxylase; GltA, citrate synthase; AcnA, aconitate hydratase; Amt, Ammonium transporter; Urt, urea ABC transporter; GlnA, glutamine synthetase; GlnK, NifHD-Nitrogen regulatory protein P-II; Glt, glutamate synthase; ActP, acetate permease; PTS, phosphotransferase systems; Nuo, NADH-ubiquinone oxidoreductase; DmsE, decaheme c-type cytochrome; CydAB, cytochrome d ubiquinol oxidase; SDH, succinate dehydrogenase; Cyt bc1, cytochrome bc1-type ubiquinol oxidoreductase; Cyt bd, bd-type cytochrome oxidase; For genes present in sulfur disproportionation and WL pathway, see Figure 2 and Figure S6.

865   **Figure 4.** Major differential genes between *Candidatus* Desulfobulbus rimicarensis and closely
866   related free-living *Desulfobulbus* strains based on the Bacterial Pan Genome Analysis.

867

868   **Figure 5**. Hypothetical model of the sulfur cycle in the gill chamber of *Rimicaris exoculata*
869   showing a syntrophic cycling of oxidized and reduced sulfur compounds between
870   sulfur-disproportionating *Deltaproteobacteria* epibionts, and sulfur-oxidizing epibionts, including
871   *Campylobacteria* and *Gammaproteobacteria*. Abbreviations: POSCs, partially oxidized inorganic
872   sulfur compounds; Cyt, cytochrome; Hyd, hydrogenases; Sqr, sulfide-quinone oxidoreductase;
873   Apr, adenylylsulfate reductase; Dsr, dissimilatory sulfite reductase; Nrf, cytochrome c nitrite
874   reductase; Nif, nitrogenase.

875

876   **Table 1.** General genomic features of *Candidatus* Desulfobulbus rimicarensis and its closest
877   free-living relatives.

878 **Table 1.**

879

	Candidatus Desulfobulbus rimicarensis DR15	*Desulfobulbus mediterraneus* DSM 13871	*Desulfobulbus japonicus* DSM 18378	*Desulfobulbus propionicus* DSM 2032
Completeness	draft	draft	draft	complete
ANI (%)		66.77	66.62	66.53
GenBank number	Bioproject PRJNA479708	AUCW01000000	AUCV01000000	CP002364
Genome size (bp)	2,921,535	4,784,586	5,794,886	3,851,869
GC Content (%)	47.3	57.6	45.8	58.9
Number of protein-coding gene	2882	3819	4802	3255
Coding density (%)	83.7	85.4	83.4	88.3
Isolation source	Hydrothermal vent shrimp	Deep-sea sediment	Estuarine sediment	Freshwater mud

880
881 **Figure 1.**

882

883

884   **Figure 2.**

885

886   **Figure 3.**
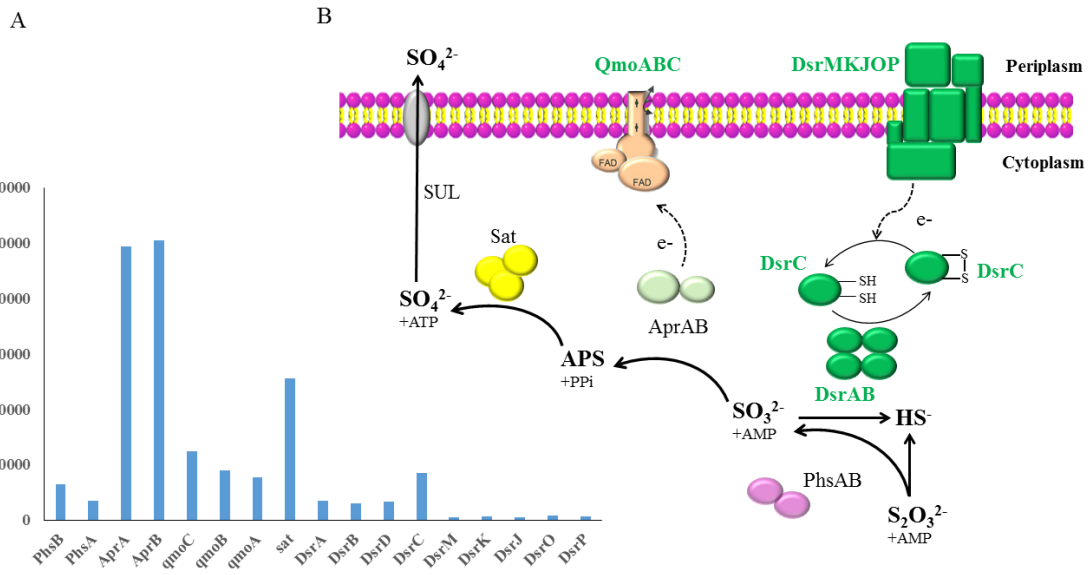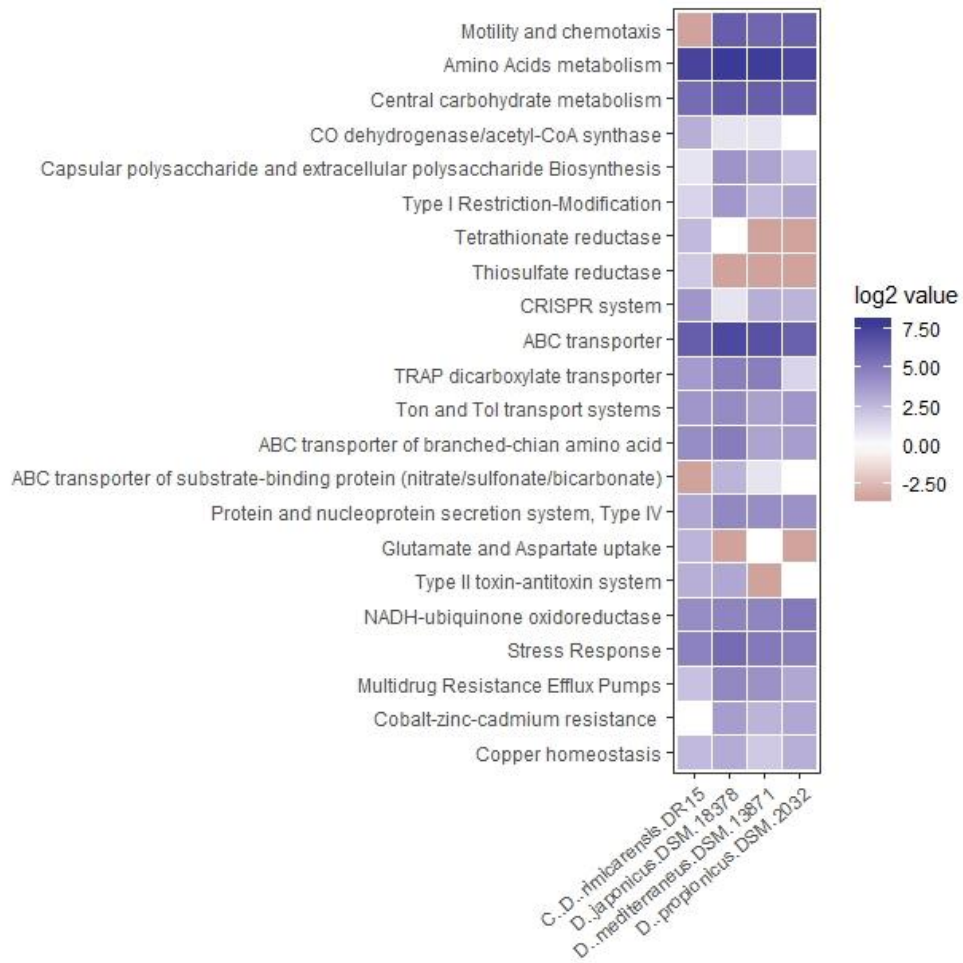
887

888 **Figure 4.**

889

890   **Figure 5.**